Micromechanics of Materials using High Energy XRD

Ersan Üstündag
Ames Laboratory and Department of Materials Science and Engineering, Iowa State University

Collaborators
Rob Rogan, Jay Hanan, Can Aydiner and Seung-Yub Lee
Department of Materials Science, California Institute of Technology

Dean Haeffner, Jon Almer, Ulrich Lienert and Doug Robinson
Advanced Photon Source, Argonne National Laboratory

Irene Beyerlein* and Sivasambu Mahesh
*Theoretical and Materials Science and Technology Divisions, Los Alamos National Laboratory

Mark Daymond
ISIS Neutron Facility, Rutherford Appleton Laboratory (U.K.)

Supported by NSF (CAREER and MRSEC), DARPA, ARO and DOE

Fracture of a Fiber Composite under Tension

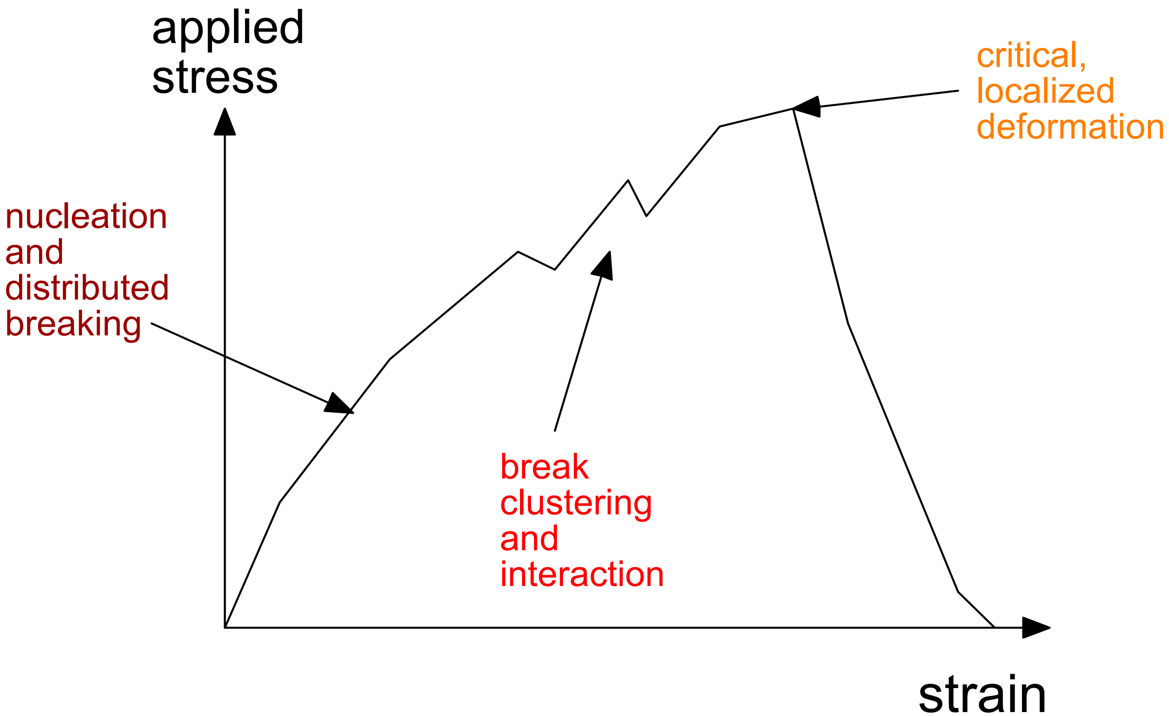

- **Aim: prediction of strength and lifetime**
- **Need: "realistic" constitutive laws**

Complications

- **Fabrication processes**
- **Inhomogeneous dislocation densities**
- **Changes in grain size**
- **Geometrical constraints**
- **Interface introduced with different properties**
- **Residual stresses**

Motivation and Approach

- Little information about deformation and constitutive behavior of materials at multiple length scales.
- Need to link experimental data with rigorous micromechanics modeling.
- Approach: Use X-ray microdiffraction to investigate deformation in materials and complement it with modeling.
- Critical issues:
  - Need for model specimens
  - “High selectivity” of diffraction
  - Only elastic lattice strains are measured with diffraction
  - Lack of “realistic” constitutive laws to calculate stress and interpret diffraction data

Advantages of XRD

- Non-destructive.
- Ability to distinguish different phases.
- Can measure elastic strain and texture.
- Simultaneous <u>strain</u> and <u>imaging</u> capability.
- Multi-scale: *nm* to *cm*.
- Deep penetration.
- *In-situ* experiment capability.

$\Rightarrow$ Determination of *in-situ* constitutive behavior

Bragg's law:

$$\lambda = 2d\sin\theta$$

Differences in lattice spacing

$\Rightarrow$ Elastic lattice strain

$$\varepsilon_{hkl}^{el} = \frac{d_{hkl} - d_{hkl}^{0}}{d_{hkl}^{0}} = \frac{d_{hkl}}{d_{hkl}^{0}} - 1$$

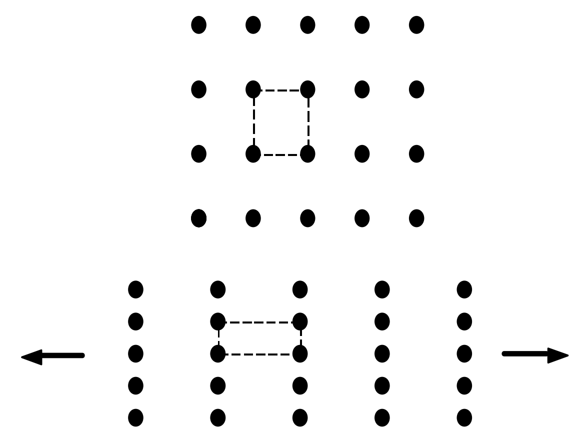

High Energy 2-D XRD Experimental Setup

Digital image plate

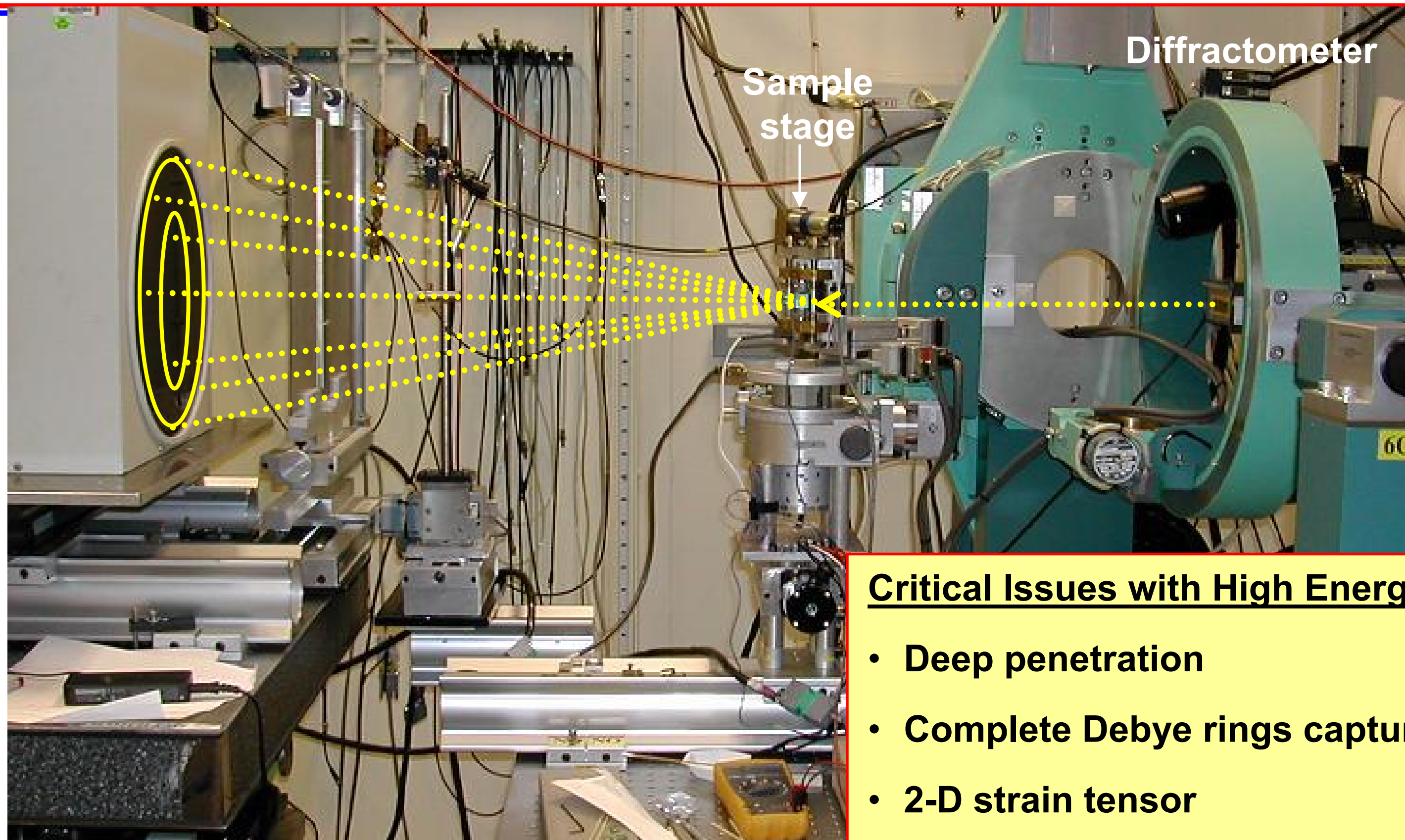

Critical Issues with High Energy 2-D XRD:

- Deep penetration
- Complete Debye rings captured
- 2-D strain tensor
- Small θ values (i.e., high strain error):
  - Sensitive to displacement error
  - Need to employ internal standard

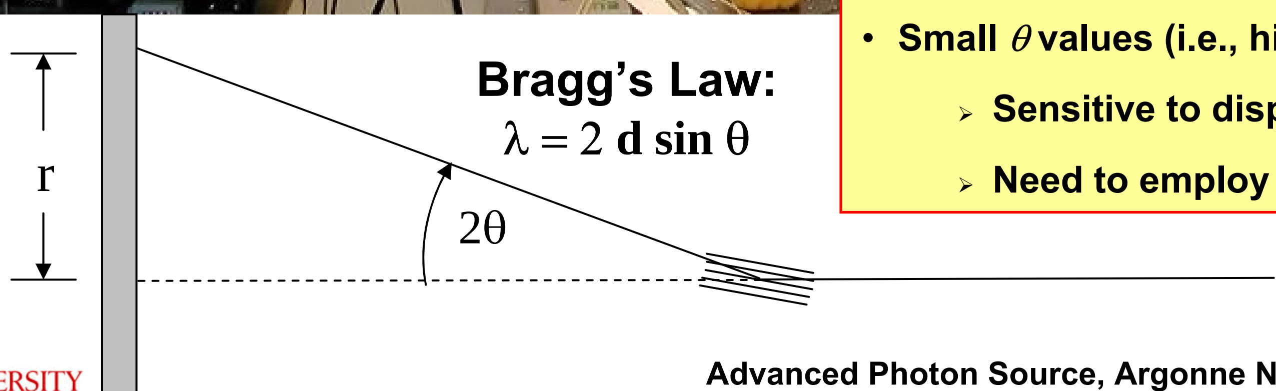

Bragg's Law:

$$\lambda = 2\,\mathbf{d}\sin\theta$$

Model Composite: Ti-6Al-4V / SiC (SCS-6)

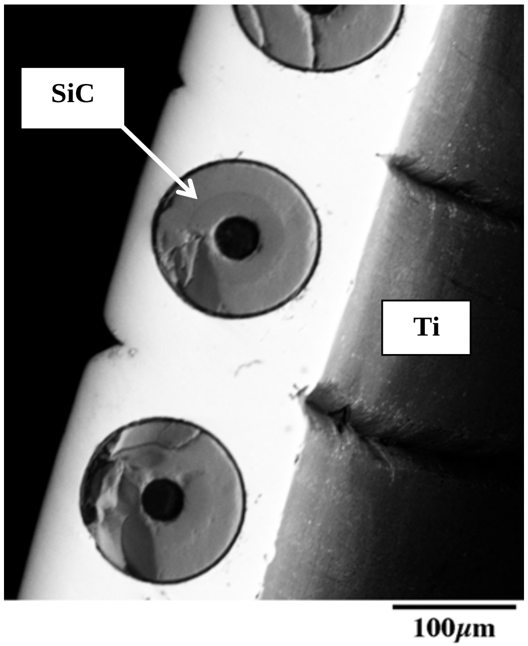

- Uniaxial tensile testing
- Damage evolution study using XRD (65 keV)
- Complete penetration
- 90 x 90 μm² spot size

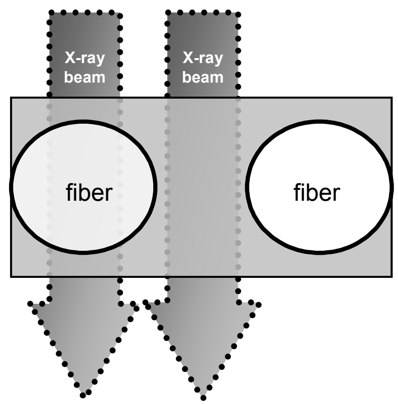

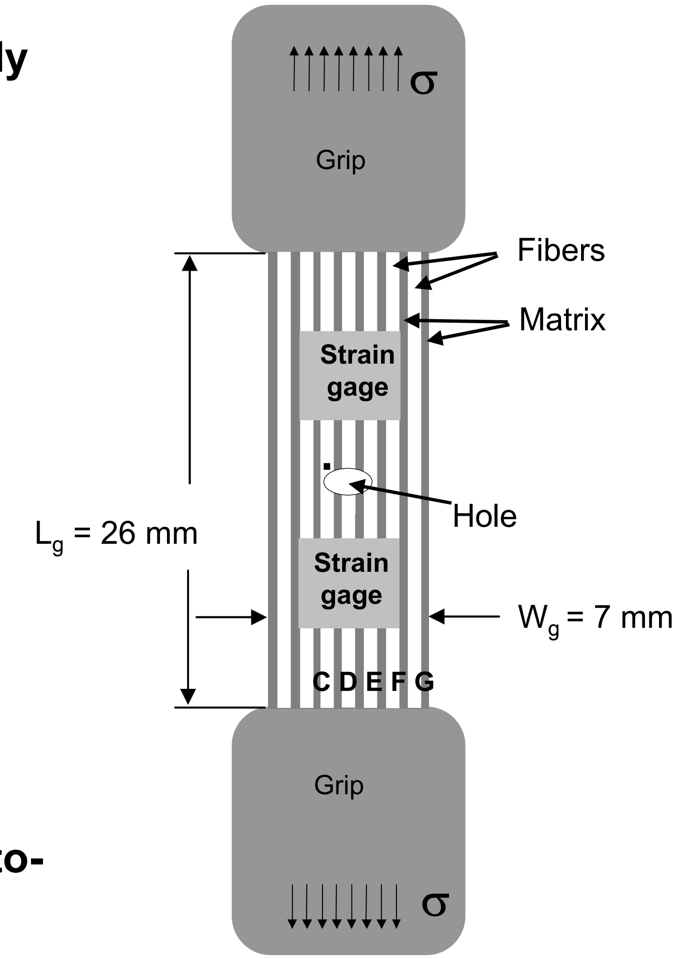

- Laminar composite: Ideal for model comparison
- 140 μm in diameter fibers; 240 μm average center-to-center distance
- 200 μm thick matrix
- Data collected with a digital image plate

Multi-Fiber Deformation Model*

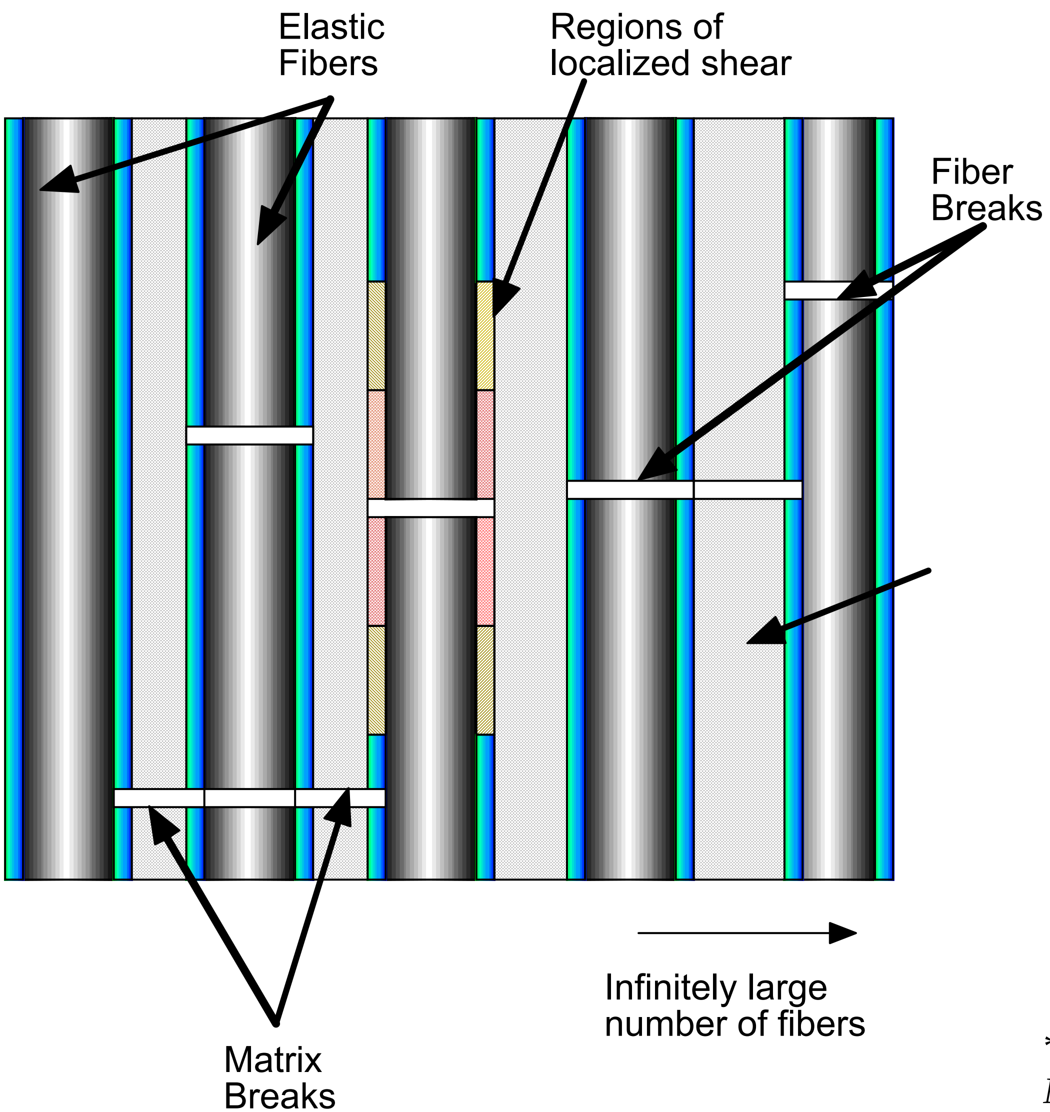

- Shear lag model for 2-D fiber composites
- Accounts for matrix sustaining elastic tensile and shear stresses (*first shear lag model to do so*)
- Allows for multiple fiber and matrix breaks
- Computationally *faster* for many breaks
- Assumes *elastic* deformation only

* I.J. Beyerlein and C. M. Landis, *Mechanics of Materials*, 1999; 31: 331.

Matrix Stiffness Shear Lag (MSSL) Model Predictions

(i)-intact matrix

(ii)-broken matrix

With $\rho = 0.289$ for both one and two broken fibers

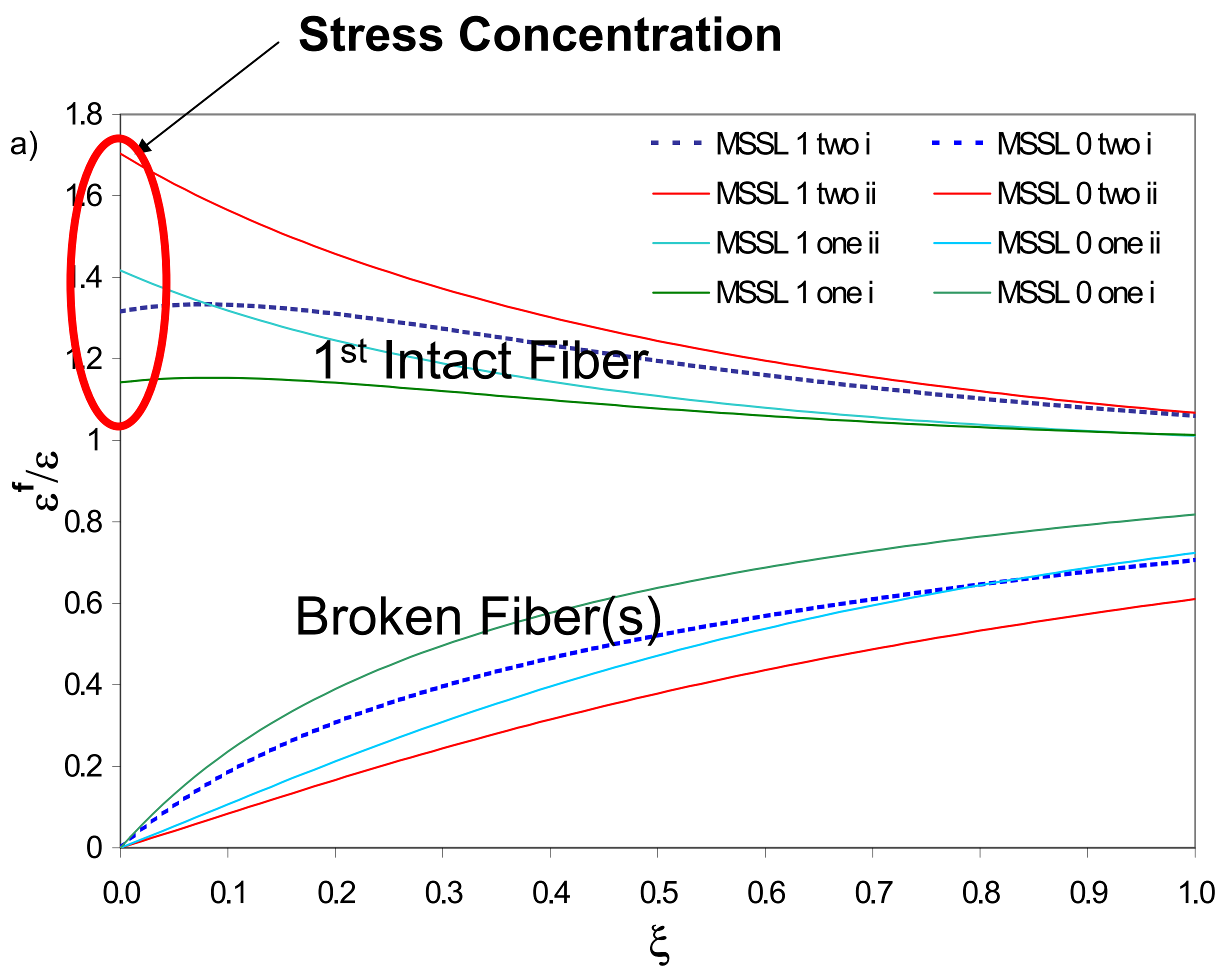

Location of Diffracting Grains

Ti (11.2) map

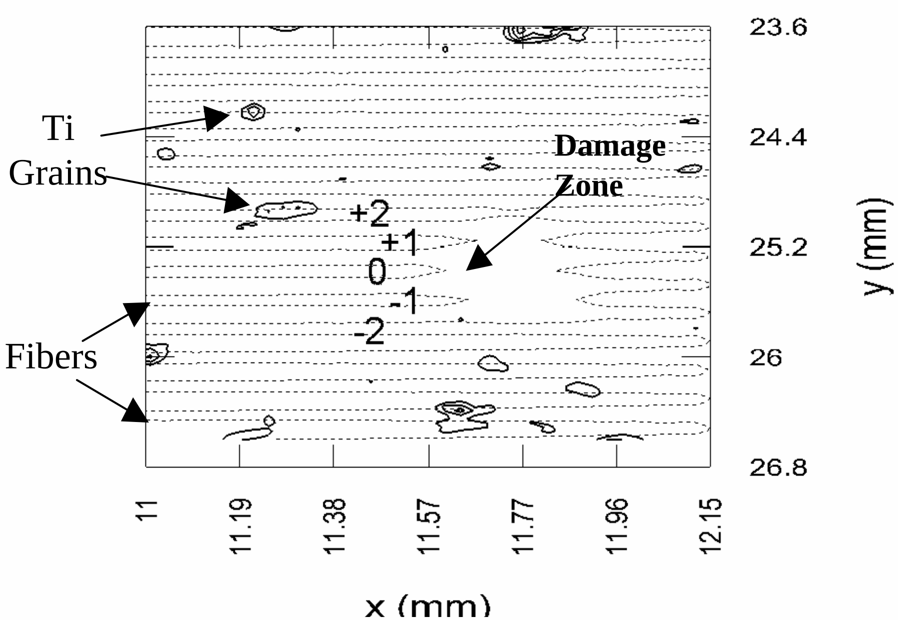

SiC (220) map

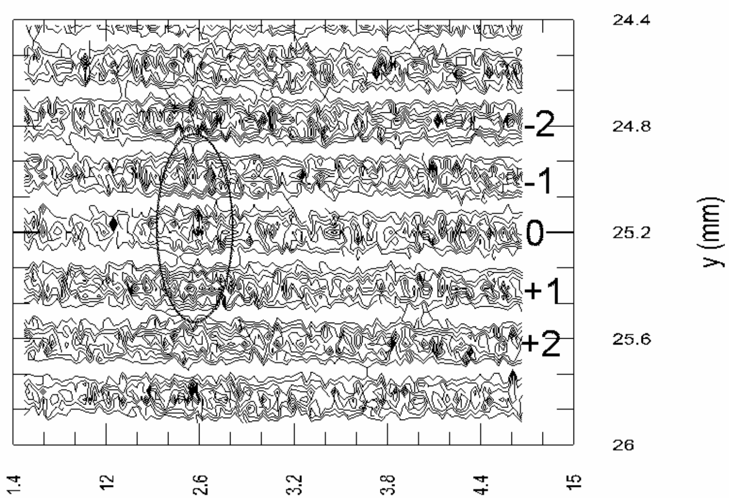

- **Ti grain size ~29 μm:**
  - **Few diffracting grains.**
- **SiC grain size ~0.2 μm:**
  - **Continuous grain map.**
- **Use of full Debye rings to obtain more matrix data.**

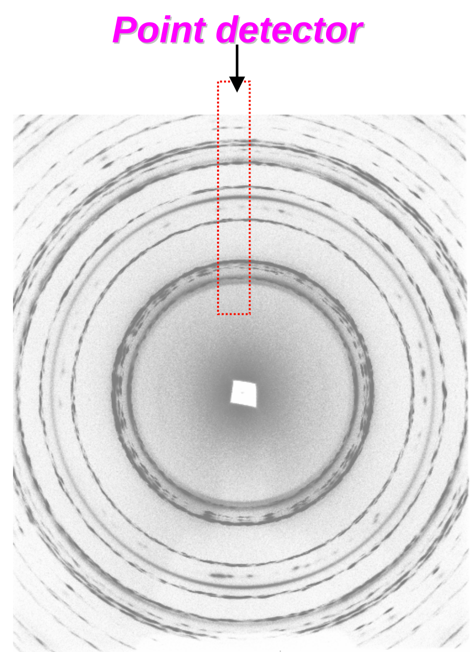

Finite Element Predictions

Ti-SiC

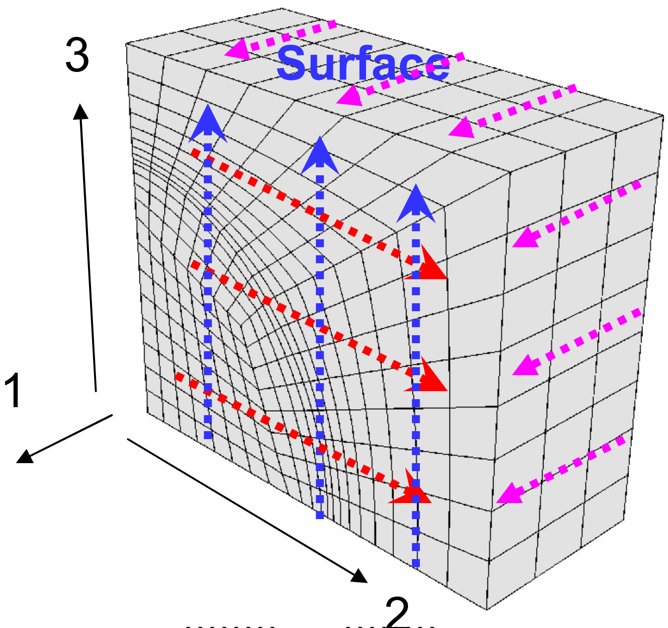

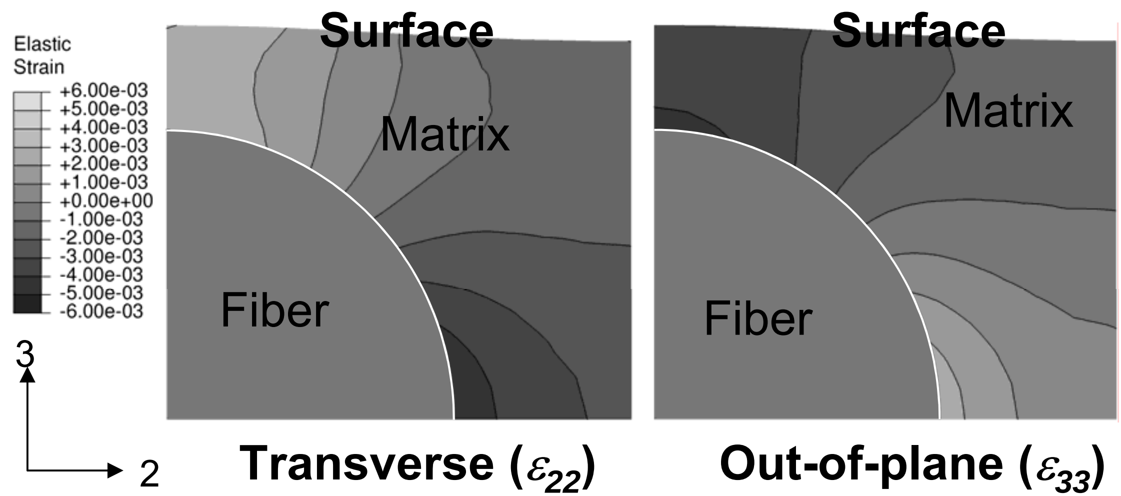

Transverse (ε_{22})

Out-of-plane (ε_{33})

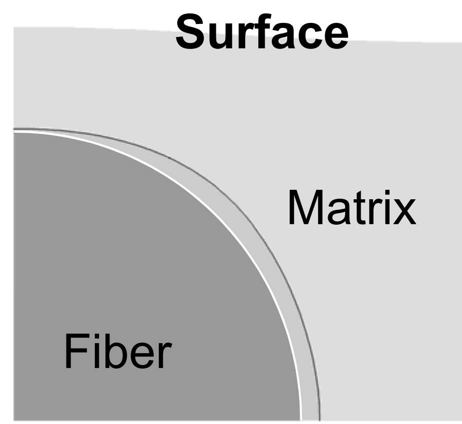

Axial (ε_{11})

- **The ... dic ... xial strains are ideal for str ... ave ... d by XRD.**
- **... l stresses (ax ... –7 ... MPa ... e fibers + ... P ... matrix**

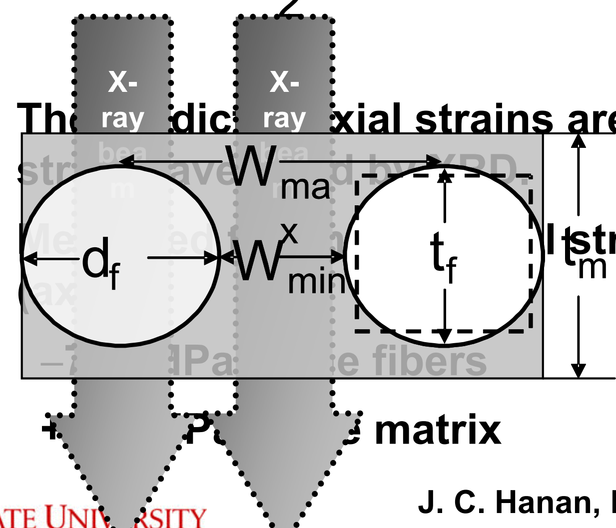

J. C. Hanan, E. Üstündag *et al*, *Metall. Mater. Trans.* 33A, 3839-3845 (2002).

Unloading Strains in Fibers Compared to the MSSL Model

Ti-SiC

Left Side of the Damage Zone:

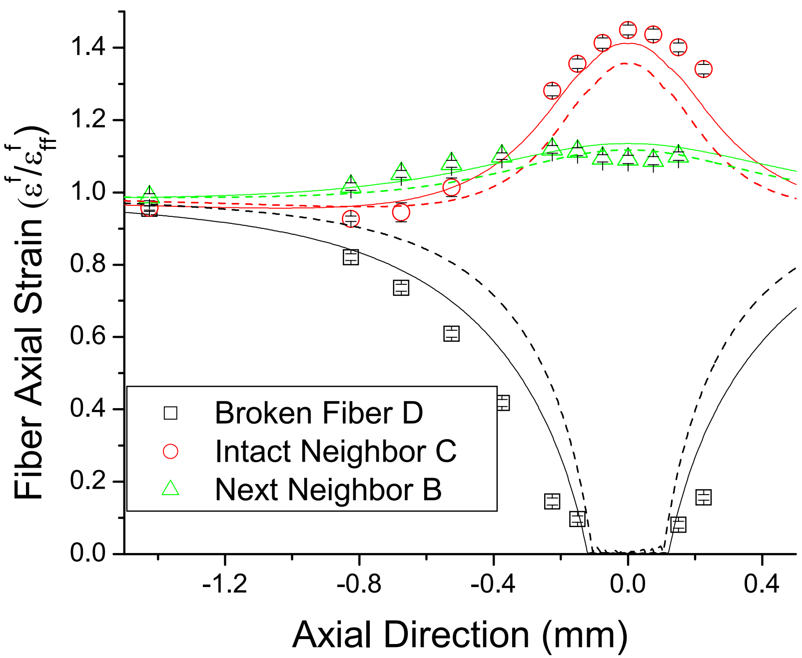

Right Side of the Damage Zone:

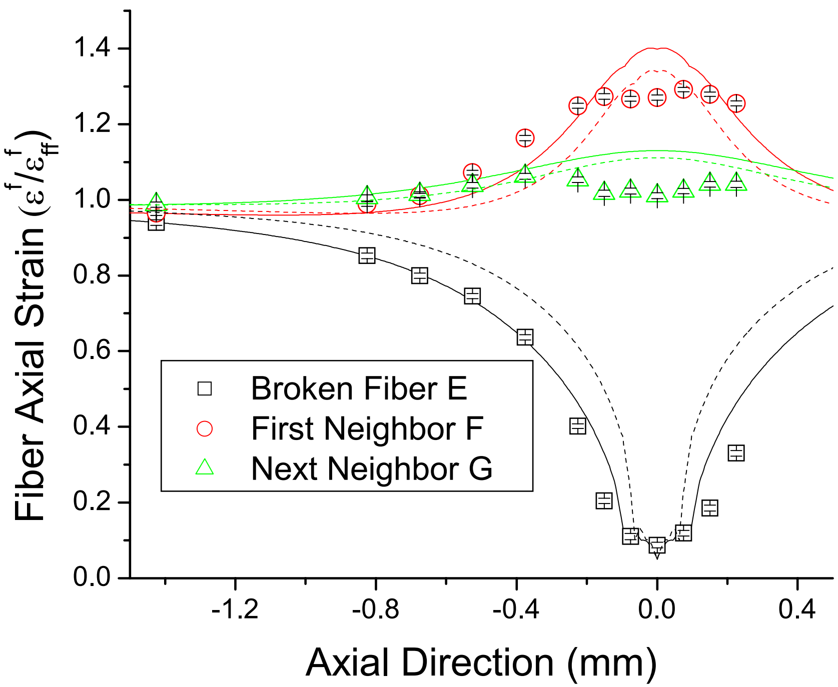

- **Good fit with 'intact matrix' case.**
- **Unloading strains were used due to plasticity in matrix.**
- **Right hand side data suggests interface debonding.**

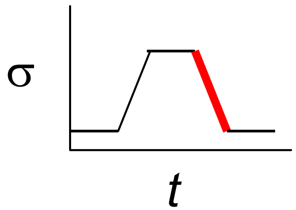

J. C. Hanan, E. Üstündag *et al*, *Acta Mater*. 51 [14], 4237-4248 (2003).

Unloading Strains in the Matrix Compared to the MSSL Model

Ti-SiC

Matrix between two intact fibers:

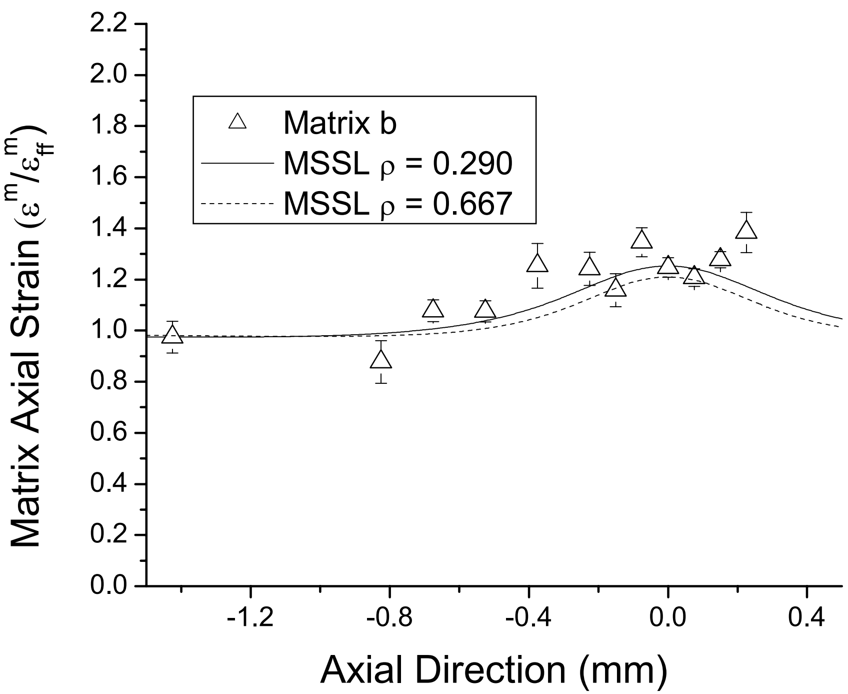

Matrix around damage zone:

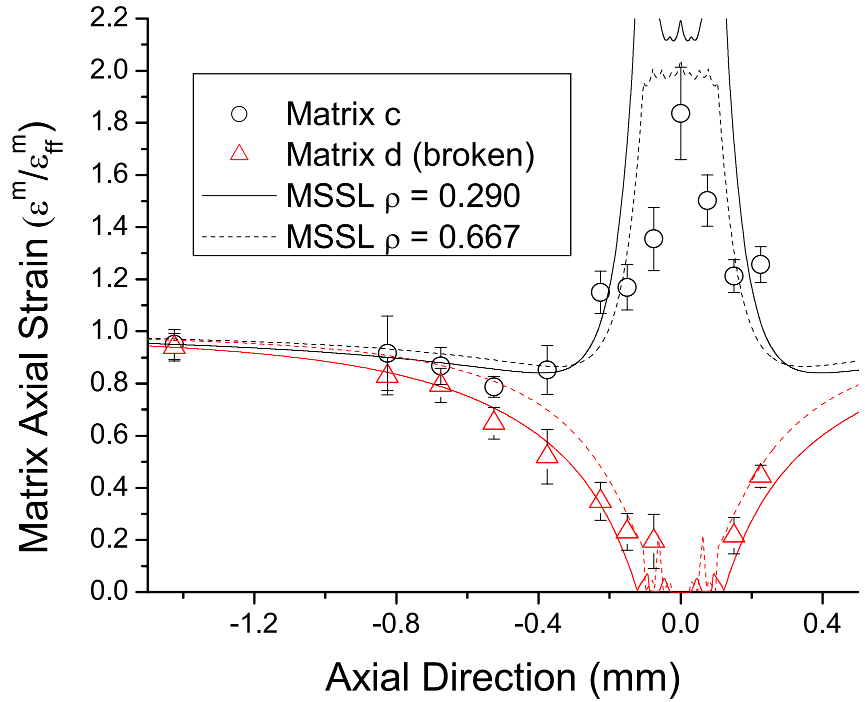

- Better fit with 'intact matrix' case.
- ρ = 0.290 appears to be a more realistic value.
- Matrix data comes from few grains.

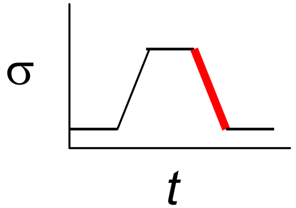

J. C. Hanan, E. Üstündag *et al*, *Acta Mater*. 51 [14], 4237-4248 (2003).

Matrix Strains Using Image Plate

Ti-SiC

Axial Strain Map

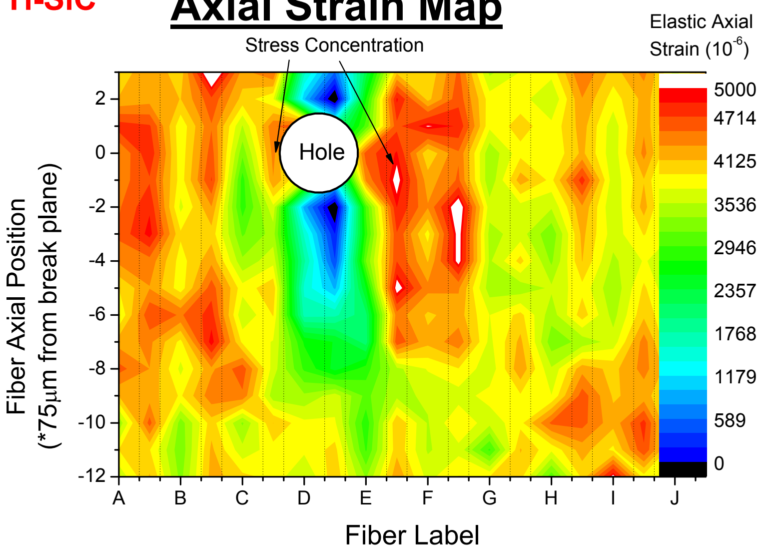

Shear Strain Map

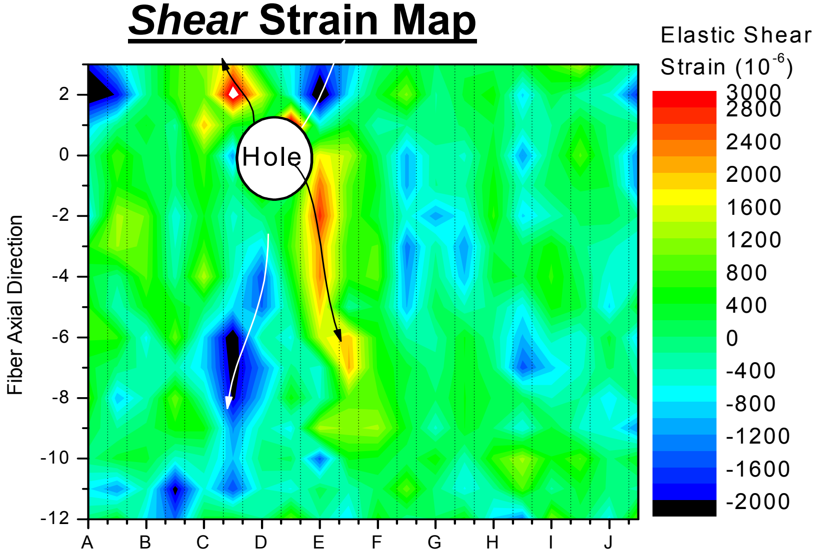

Transverse Strain Map

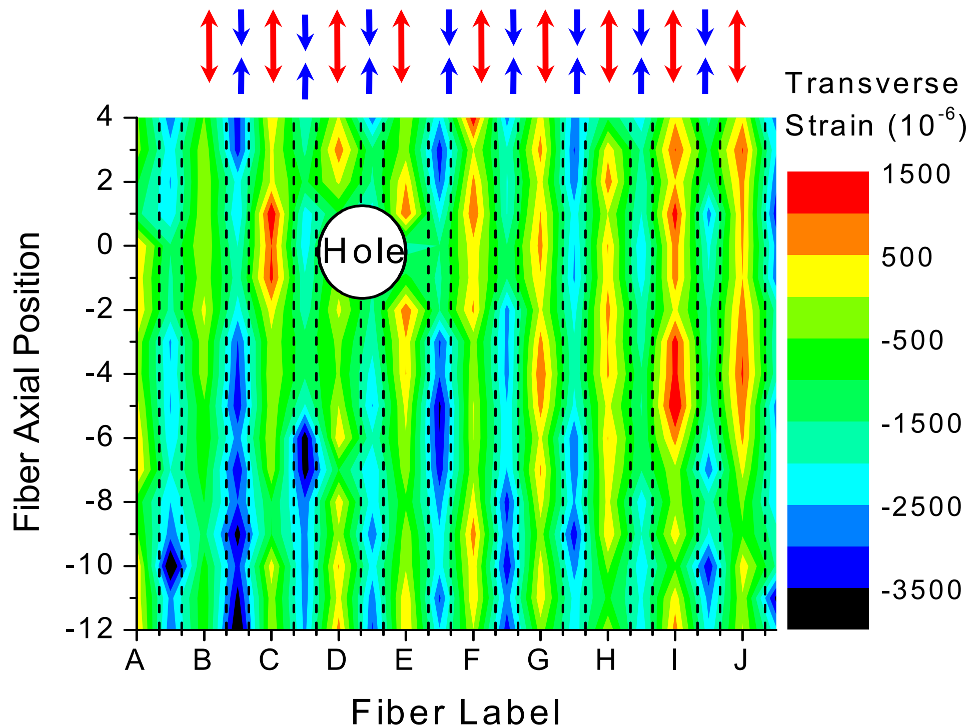

- Multi-axis strain data
- Significant strain concentrations in matrix

σ = 850 MPa

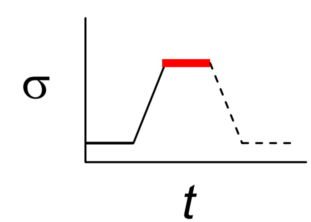

Transverse Thermal Residual Strain from FEM

Ti-SiC

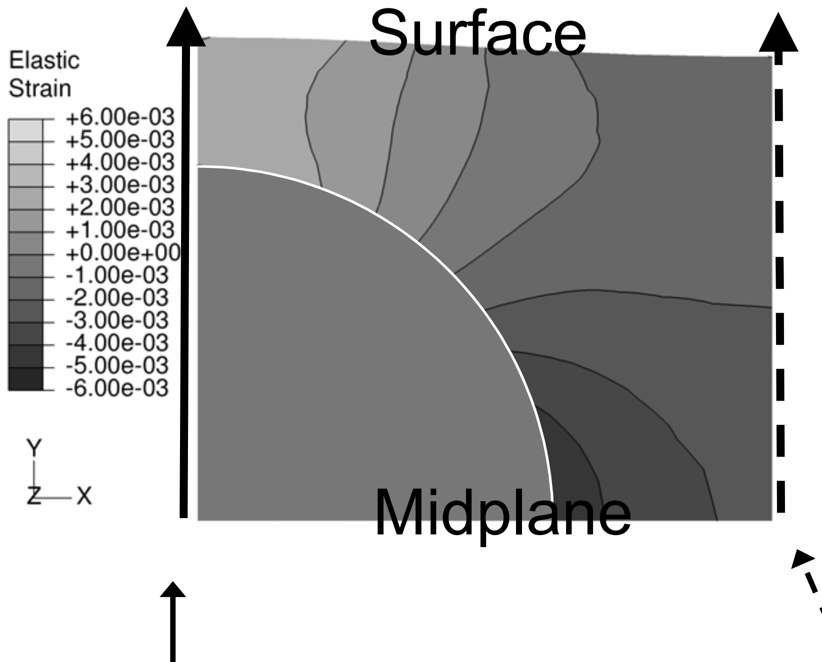

- Tension over the fibers.
- Compression between fibers.

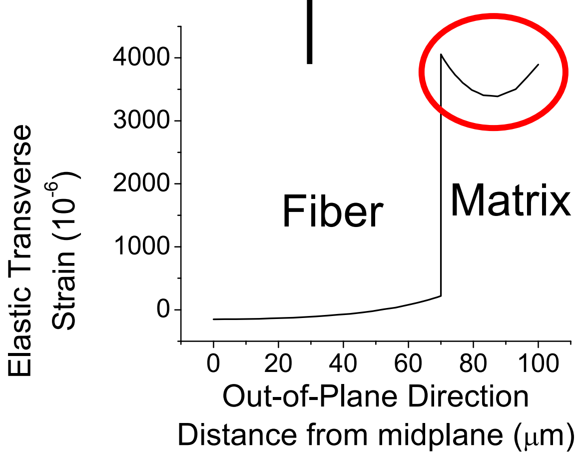

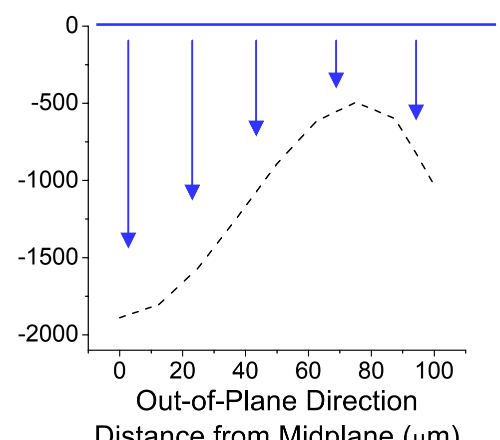

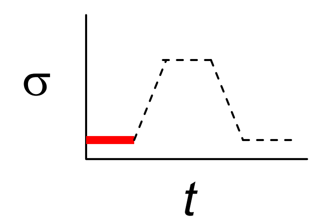

<u>Change</u> in Matrix *Axial* Residual Strain due to Loading

Ti-SiC

- **The compressive regions identify <u>*plastic*</u> deformation while loading the composite**

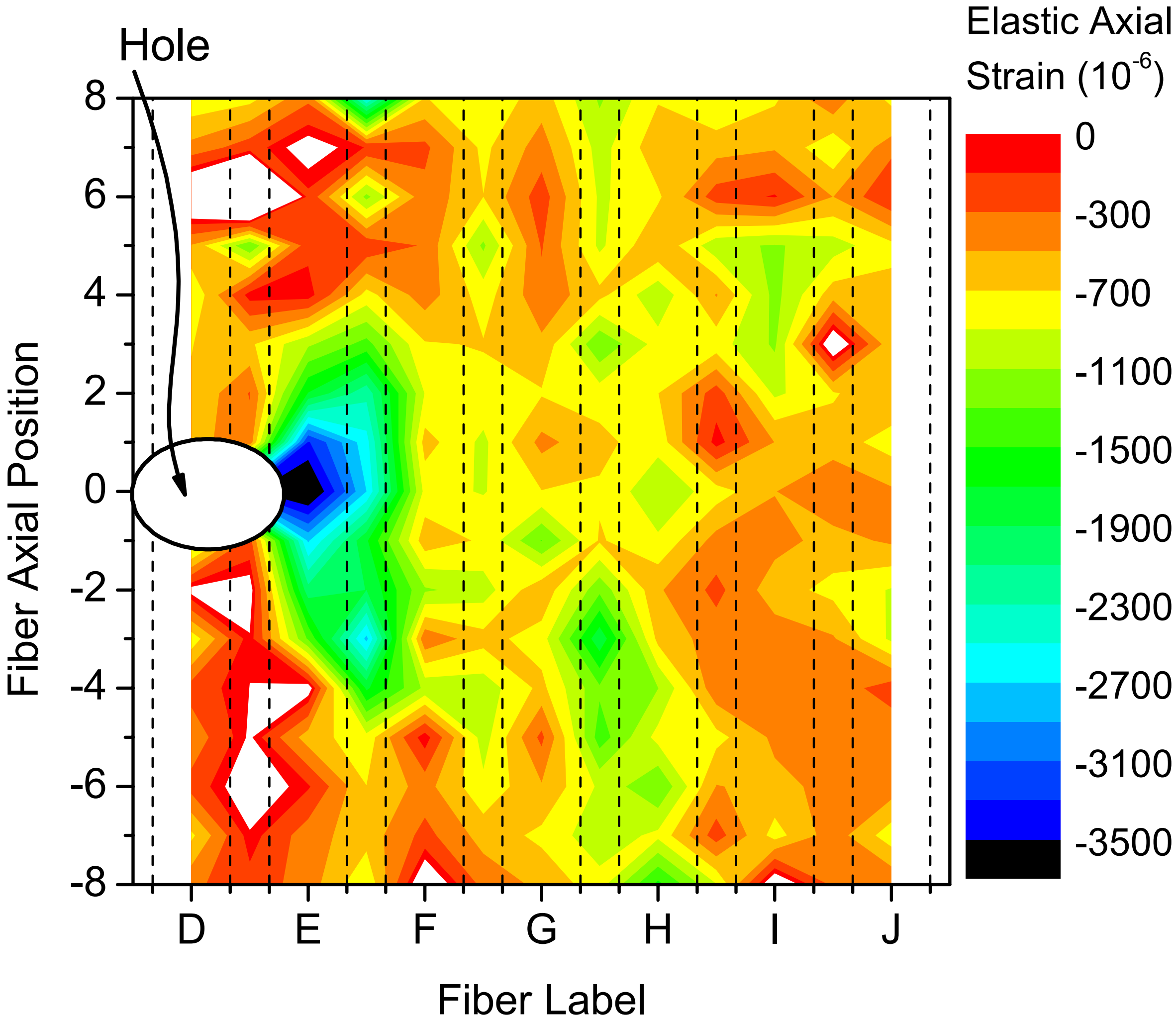

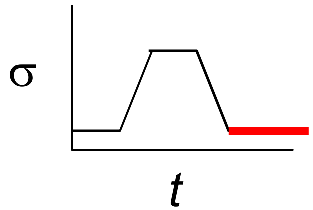

Micromechanics of Composites: *Conclusions*

- **High energy XRD allows rigorous validation of advanced micromechanics models.**
- **Detailed stress/strain and structure data can be collected at the microstructure scale.**
- **Possibilities now exist for extensive studies under various loading conditions.**
- **Composite field will benefit tremendously from combined diffraction and imaging capabilities.**

Constitutive Behavior of Ferroelectric Materials

$PbTiO_3$

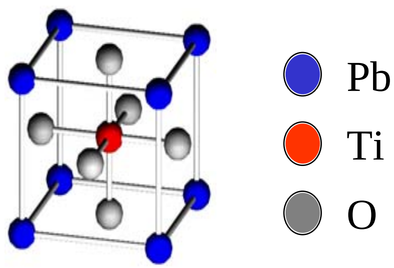

High temperature
(non-polar cubic)

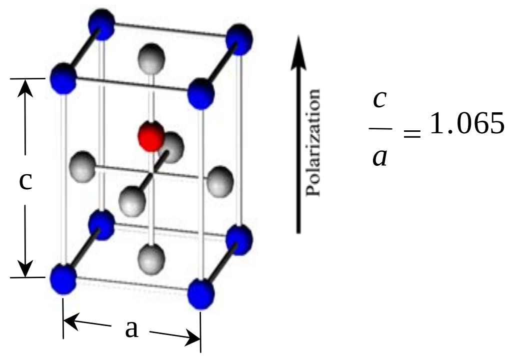

Room temperature
(<001> polarized tetragonal)

Six equivalent <001>$_{cubic}$ directions give six equivalent states at room temperature

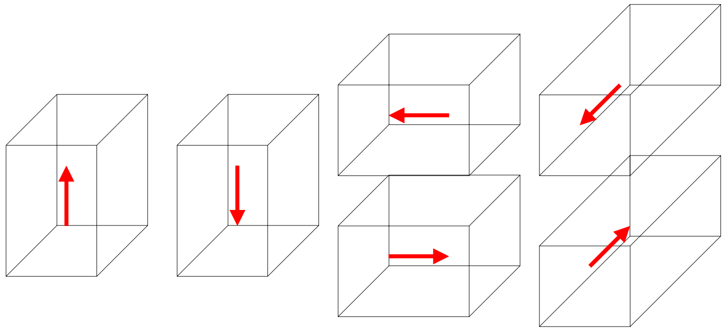

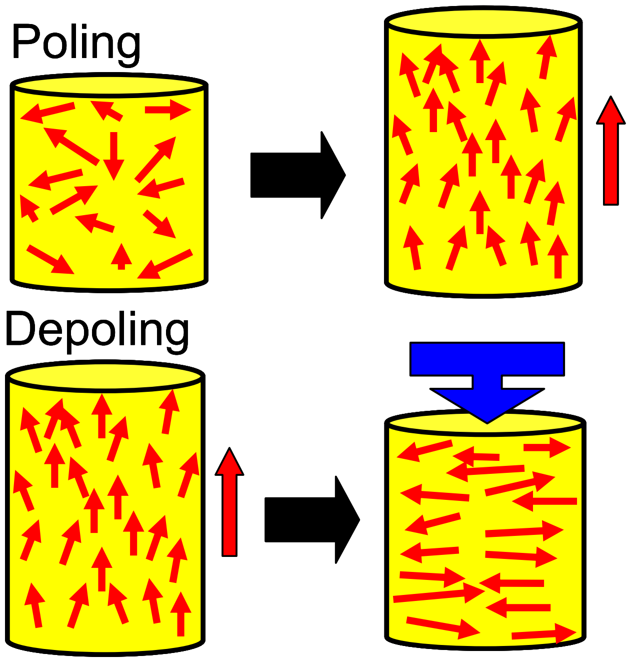

- Poling in large electric fields aligns crystallite polarizations through a process called "ferroelectric switching".
- Applied stress causes de-poling and 90° domain switching.
- Fundamental understanding of the details of domain micromechanics is crucial for accurate modeling of ferroelectrics.

Self-Consistent Modeling of Ferroelectrics

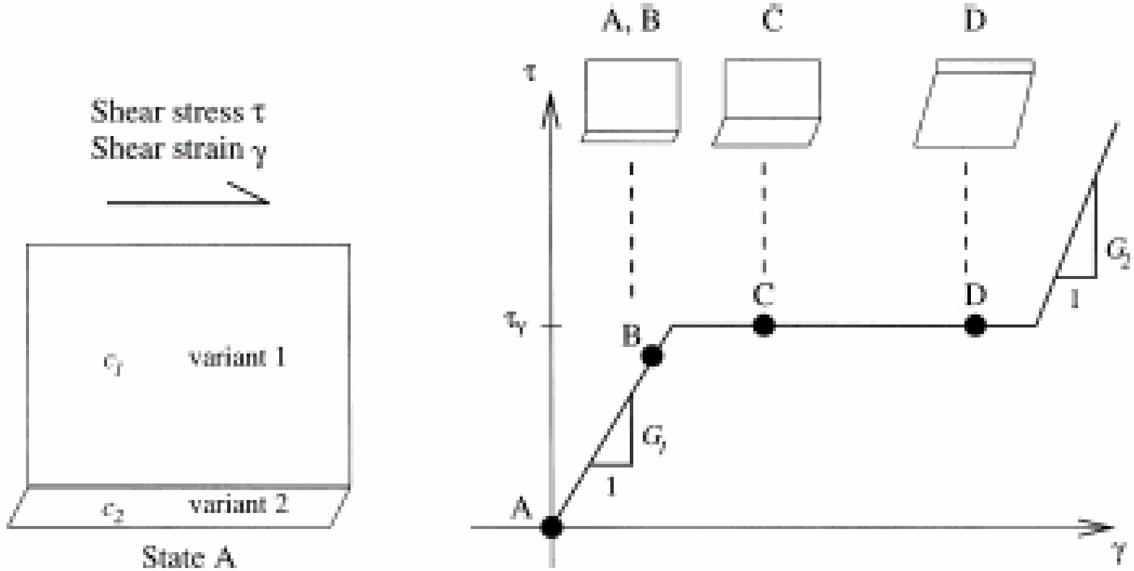

Fig. 2. The progressive nature of ferroelectric transformation within a crystal due to domain wall motion.

- **Domain switching within a single crystal (grain).**
- **Each of *M* (=6) variants can transform into any of the remaining *M-1* (=5) variants: total of 30 transformations (90° and 180 ° switches).**
- **Domain wall motion is dissipative (similar to dislocation motion).**
- **Stress (σ_{ij}) and electric field (E_i) are uniform in the crystal.**
- ***There is no hardening*.**
- **Dislocation plasticity is neglected.**

Huber, J.E., Fleck, N.A., Landis, C.M. and McMeeking, R.M., *J. Mech. & Phys. Sol.,* **47** (1999) 1663-1697.

Constitutive Behavior of Polycrystalline $Pb(Zr,Ti)O_3$

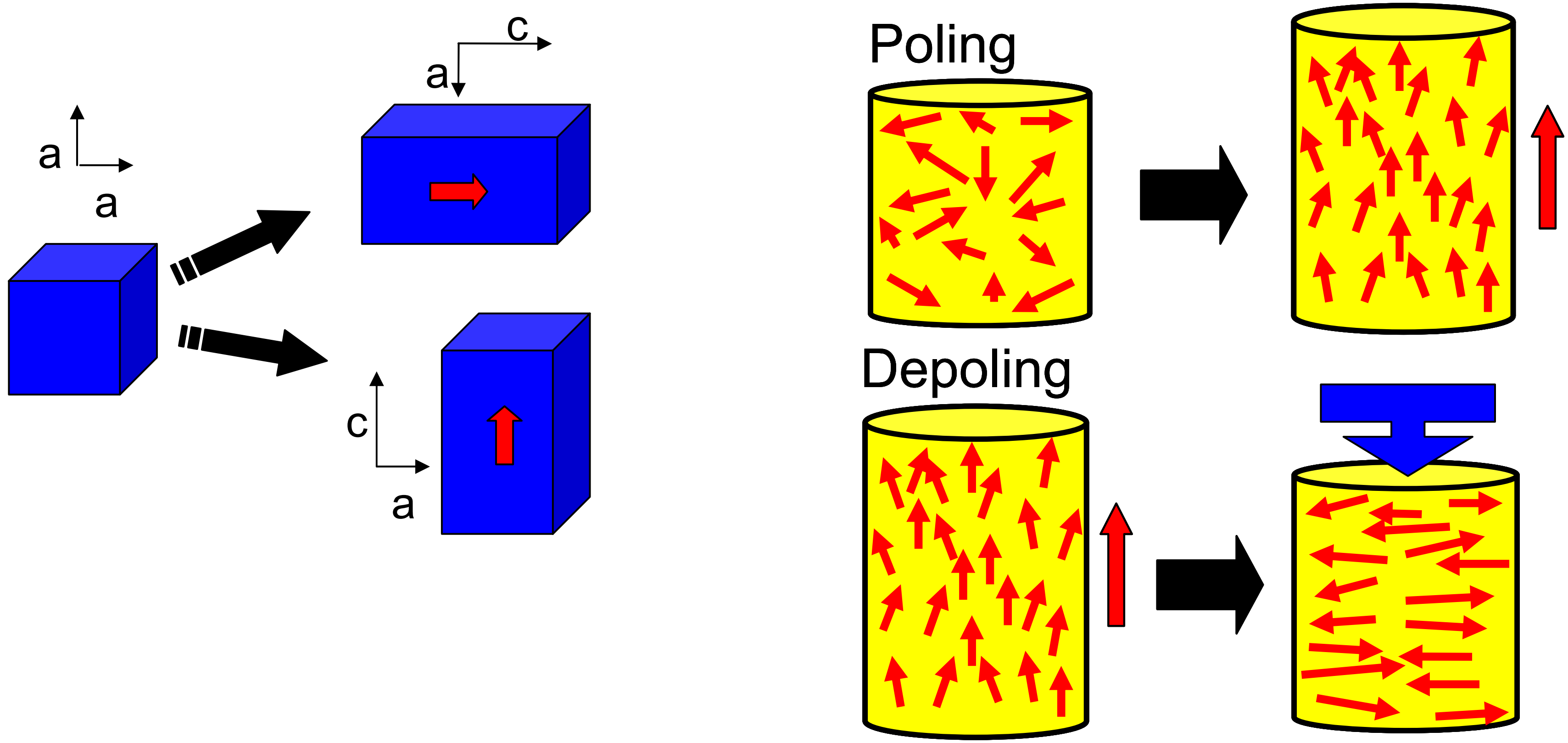

- **Studied electromechanical response of polycrystalline $Pb(Zr,Ti)O_3$**
- **Employed neutron diffraction and high energy XRD**
- **Diffraction yields *hkl* dependent strains and texture data, information crucial for modeling**

Neutron Diffraction: Lattice Strain Evolution in Two Phase $Pb(Zr,Ti)O_3$*

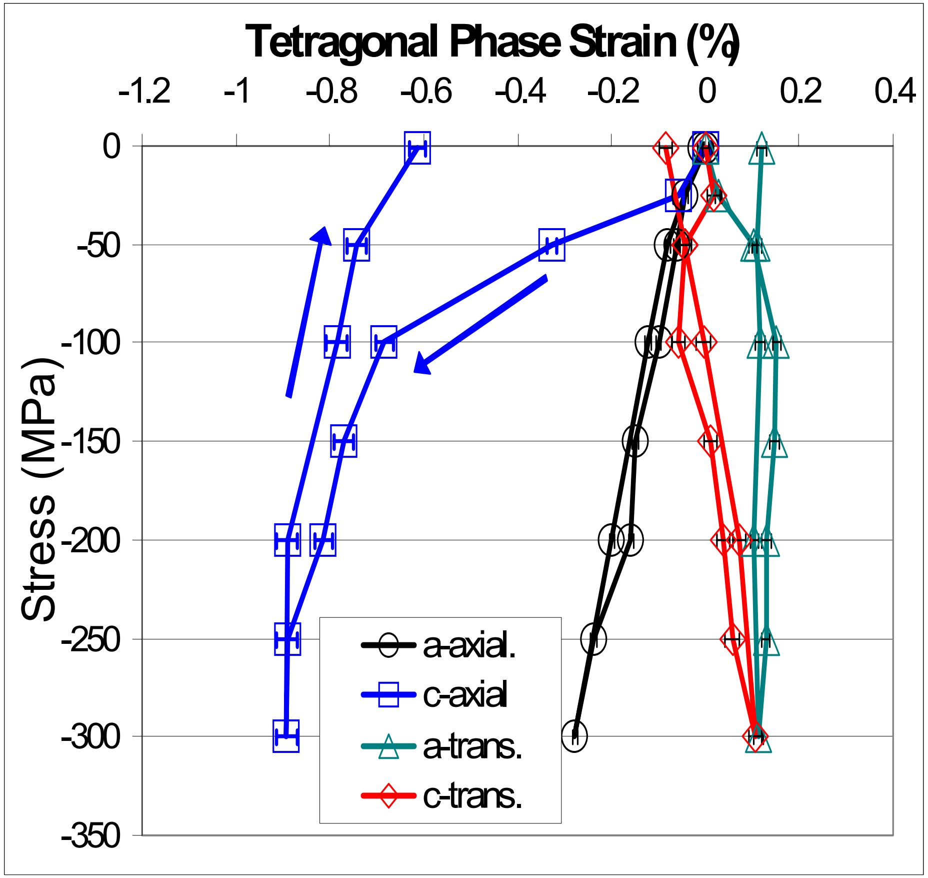

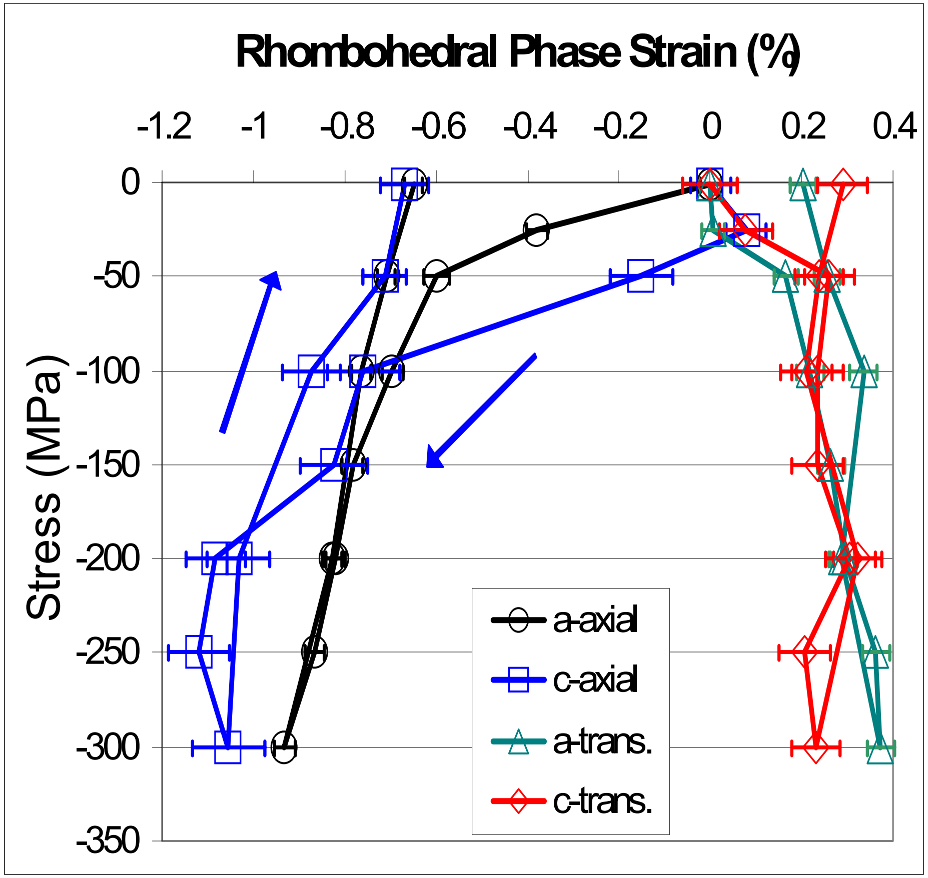

* **R.C. Rogan, E. Üstündag, B. Clausen, M.R. Daymond, *J. Appl. Phys.* 93[7], 4104-4111 (2003).**

Neutron Diffraction: Experimental Setup at ISIS

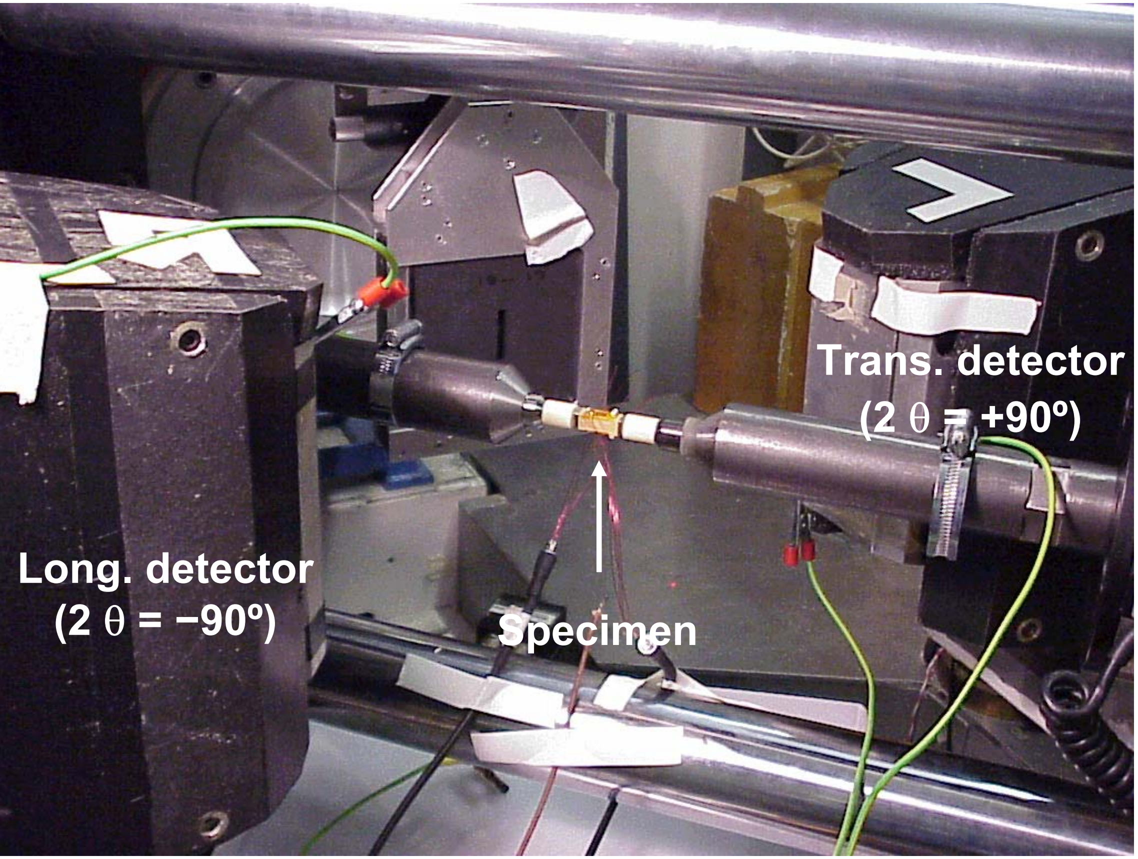

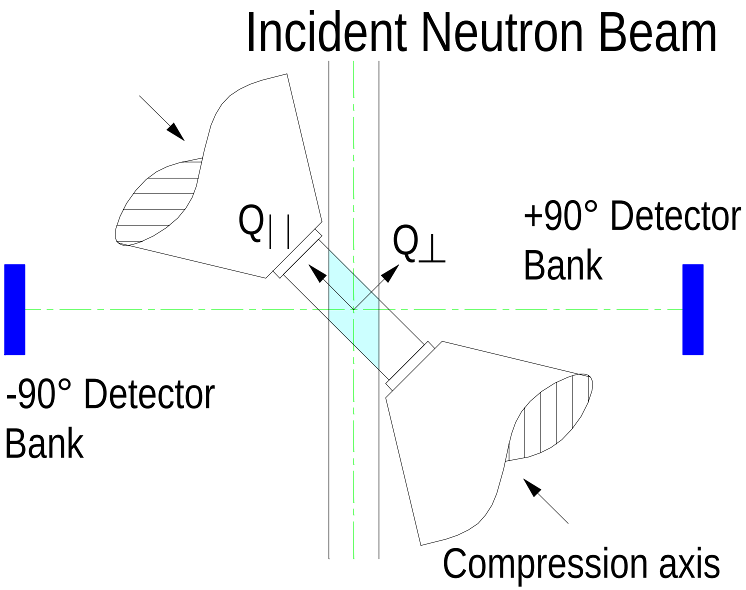

- **+90° (left) bank observes <u>transverse</u> sample behavior**
- **−90° (right) bank observes <u>axial</u> sample behavior**
- ***Very limited detector coverage and slow data collection***

High Energy XRD at APS Sector 1: 2-D Data

- Samples were electrically poled under sequentially increasing static fields while taking X-ray patterns.
- Results indicate a severe dependence on *η* and a critical coercive field of ~0.3 kV/mm.

Poling Strains as a Function of η

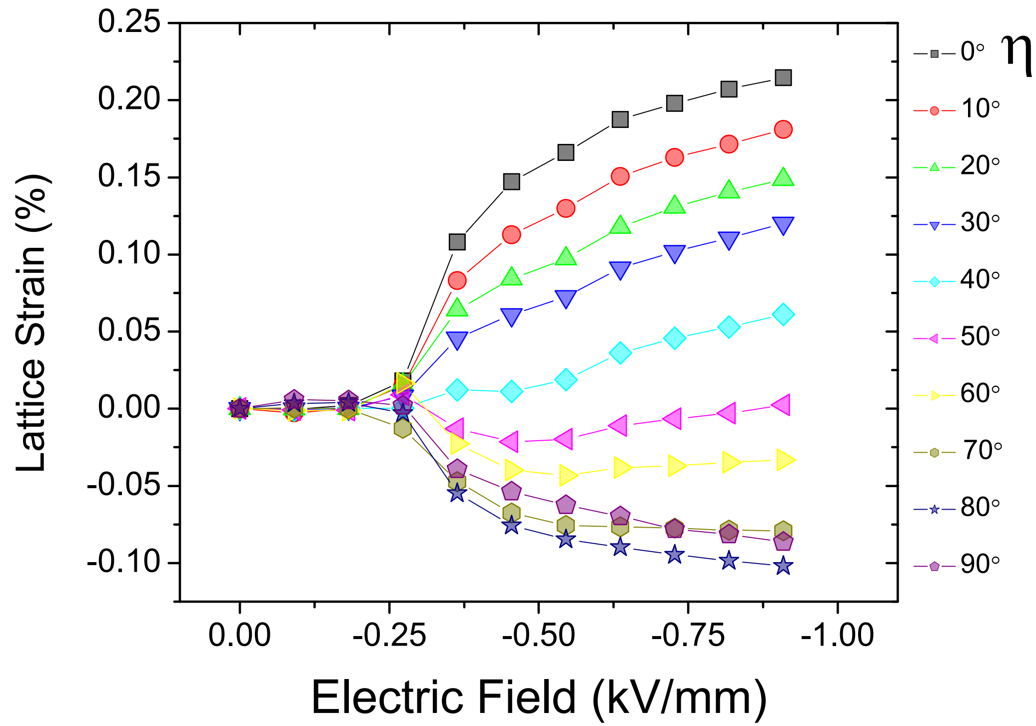

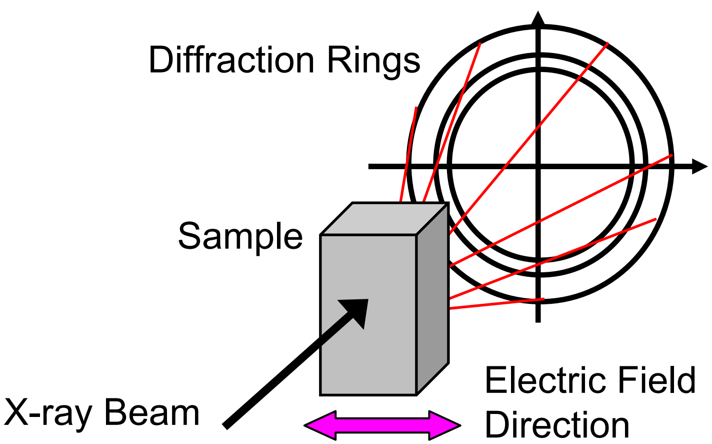

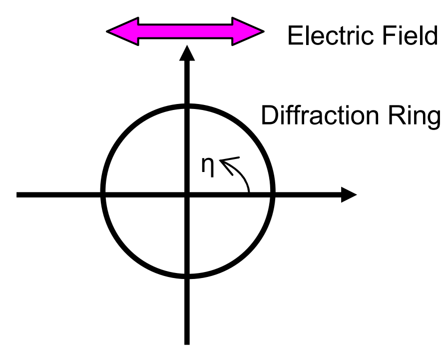

High Energy XRD at APS Sector 1: 2-D Data

- After poling, samples were cycled through positive and negative ranges.
- The typical "butterfly" curve was observed for each azimuthal angle.
- By "caking" 36 virtual detectors were generated to allow a wide coverage of reciprocal space.

Response to Electric Field Cycling

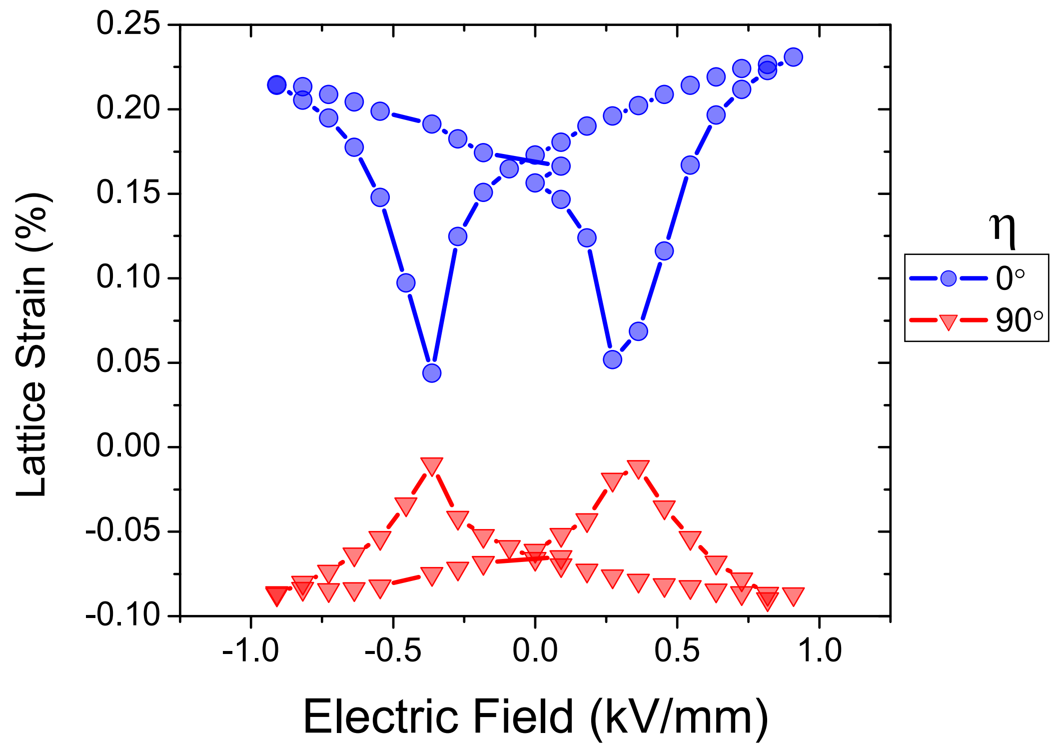

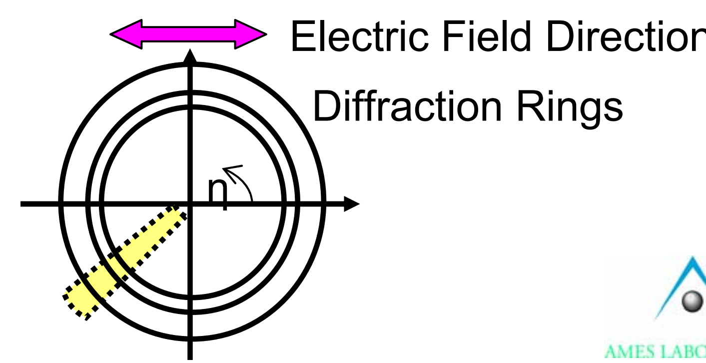

R.C. Rogan, E. Üstündag, M.R. Daymond and U. Lienert, submitted to *J. Appl. Phys.* (2004).

Angular Dependence of Strain Behavior

By defining various "spans" the data may be broken down as a function of angle

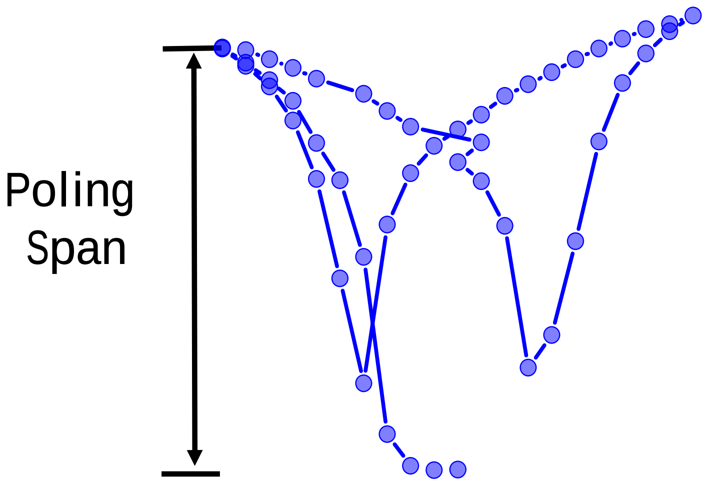

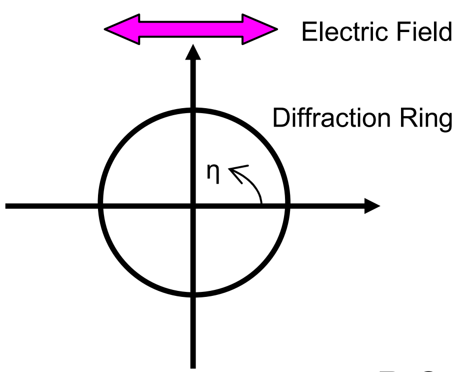

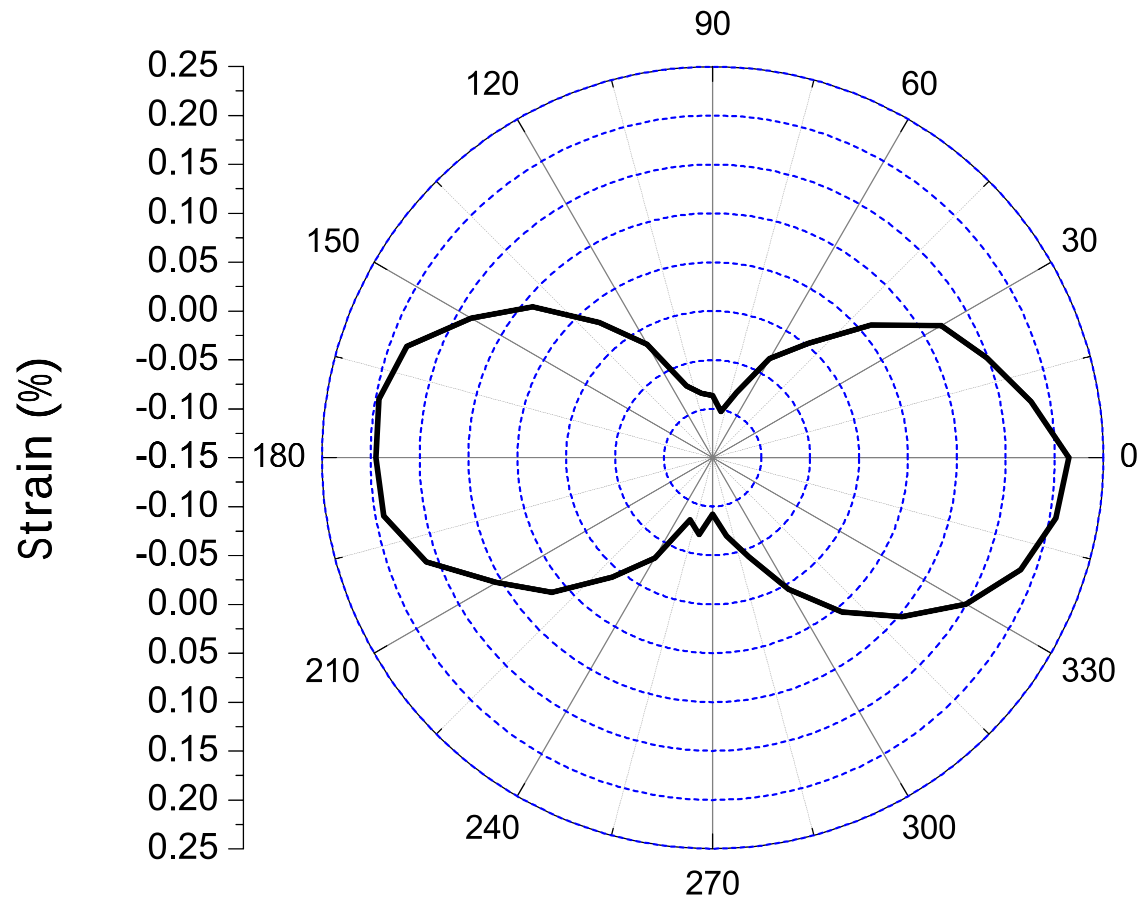

R.C. Rogan, E. Üstündag, M.R. Daymond and U. Lienert, submitted to *J. Appl. Phys.* (2004).

3-D XRD: Domains in a Single Grain of Polycrystalline $BaTiO_3$

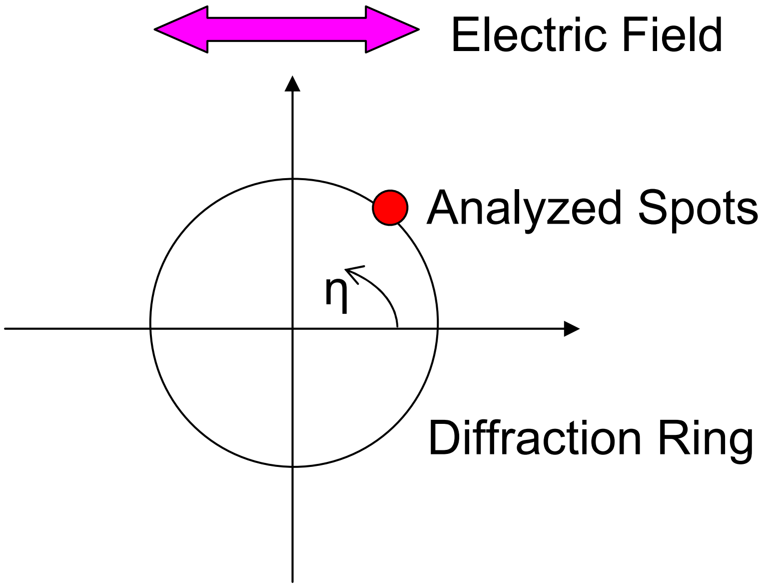

- **Cycled electric field on a pre-poled $BaTiO_3$**
- **Monitored evolution of domain volume fractions and strain within individual grains**
- **Critical information for 3-D FEM of ferroelectrics**

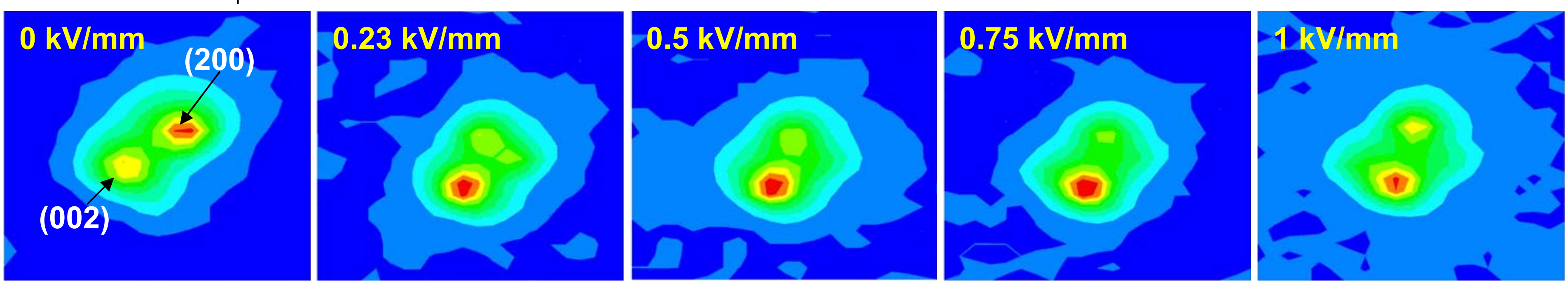

- **Domain switching occurs at a low field (E_c ~ 0.5 kV/mm)**
- **At higher fields spot separation and rotation increases (3-D lattice strain)**

Constitutive Behavior of Ferroelectrics: *Conclusions*

- High energy XRD is ideal for micromechanics studies on ferroelectrics.
- Fast electromechanical loading allows *in-situ* investigation of constitutive response.
- 2-D strain and texture data yield multiaxial information about material behavior.
- Development of 3-D XRD capability at APS will add *mesoscale* capability.
- It is possible to perform detailed multiscale, multiaxial studies of ferroelectric micromechanics at APS.